

Improved magnetic behavior of hemicycle PM motor via stator modification

Kwang T. C., Mohd Luqman Mohd Jamil, Auzani Jidin

Power Electronics and Drive Research Group (PEDG), Universiti Teknikal Malaysia Melaka, Malaysia

Article Info

Article history:

Received Sep 26, 2019

Revised Dec 9, 2019

Accepted Jan 31, 2020

Keywords:

Hemicycle stator

PM motor

Weight reduction

ABSTRACT

This article presents the simple basic sizing approaches to decrease overall weight of motor and improve magnetic characteristics in PM motor. A review on various stator design in PM motor i.e. radial-flux or axial-flux with slotted or non-slotted is presented. As magnetic and electric loading influence the electromagnetic motor performance, modification on stator body are included in investigation for a desired electromagnetic torque performance. Influences of tooth body width sizing and additional stator slots sizing in PM motor equip with hemicycle stator design are carried out. Two designs are included, both having similar semi-circle stator but different in additional slot tooth within and over 180° i.e. Design 2 and 3 respectively. For optimization using 2D-Finite Element Analysis, optimal tooth body sizing and additional stator tooth result the weight significantly reduce by 44%, 5.9 Nm output torque and 30% torque ripple.

*Copyright © 2020 Institute of Advanced Engineering and Science.
All rights reserved.*

Corresponding Author:

Mohd Luqman Bin Mohd Jamil,
Power Electronics and Drives Research Group (PEDG)
Universiti Teknikal Malaysia Melaka,
Hang Tuah Jaya, 76100 Durian Tunggal, Melaka, Malaysia
Email: luqman@utem.edu.my

1. INTRODUCTION

According to National Electrical Manufacturers Associations (NEMA), Permanent magnet (PM) motors are electronically commutated and required three phase inverters for a desired rotational [1]. Due to high torque density, high efficiency, reliability and lightweight structure, PM motors become a favourable choice in high-torque low-speed application compares to Brushed DC motors and Stepper motors [2-6]. Recently, electric machines have benefit mankind in handling variation specific tasks due to disability of labour wear. However, some application faced bulky size, high density, low torque density and high-power consumption. In [7, 8], investigation on axial flux orientated design, drive train and parametric design in PM motors are presented to overcome these parasites. A comparative study between single-sided and dual-sided, radial or axial flux orientation motors are presented to justify the pros and cons between these motors' topologies. Figure 1 shows the overview stator design topologies for high-torque low-speed technologies.

Conventionally, radial-flux PM motors configure with single-side design, slotted or slotless are made up stacked steel laminations and copper coil wound among slot stator body. By having a proper of stator slots sizing, slotted configuration results high electric loading, torque density, efficiency, output average torque and cheaper compare to slotless type [9-10]. However, high cogging torque, acoustic noise and vibration is inevitable. Therefore, variation stator design i.e. non-slotted, skewing, dummy slots, notch slots and fractional slot configuration is considered for low cogging torque and minimum torque ripple [11]. Recently, high output torque and power density in radial flux orientated is a must to achieved desired performance. In this case, double-sided of RFPM is preferable where the motors is configured with dual-rotor and single-stator or dual-stator and single-rotor configuration. For dual rotor topology, the motors are constructed with two permanent magnets in single rotor i.e. outer stator surface and inner stator surface.

These configuration results low copper quantity, high efficiency and high torque density by double compare to conventional stator design [12, 13]. Yet, these motors face high complexity, torque ripple and bulky volume [14].

While dual stator design is configured with single constant magnetic rotor and two stator (DSPM-SR) design, outer and inner stator structure. The coils are typically wound among the slots results two independent torque, high torque density and high flux linkage about doubly than conventional stator geometry [15, 16]. The investigation is then extended with variation slotted stator design such as Double Stator Arc Permanent Magnet (DSPM-AP), Double Stator Double Pole (DSPM-DP), Double Stator with Interior Magnet (DSPM-IP), Double Stator with Cup Rotor (DSPM-CR) and DSPM-SR for better torque performance i.e. torque constant density and efficiency [17]. However, high cogging torque, torque ripple, cost and complexity in manufacturing is avoidable compare to conventional slotted design. Example of various radial flux orientation in PM motors are shown in Figure 2. For rotor design as shown in Figure 3 [18], the rotor is made up of Neodymium Iron Boron (NdFeB) permanent magnet and can be magnetize i.e. parallelly and radially direction. By having a proper magnetization flux, SPM motors results high electromagnetic performance and easily to fabricate than interior permanent magnet (IPM) motors.

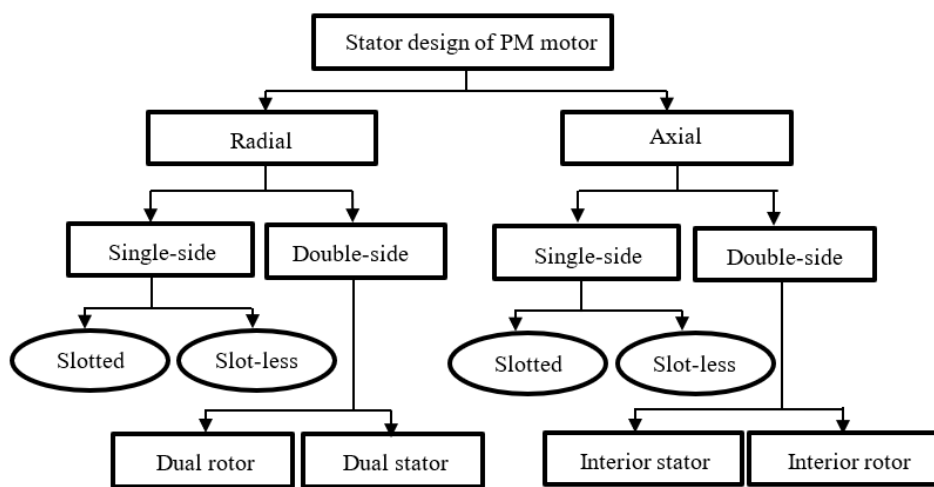


Figure 1. Overview of stator design topologies

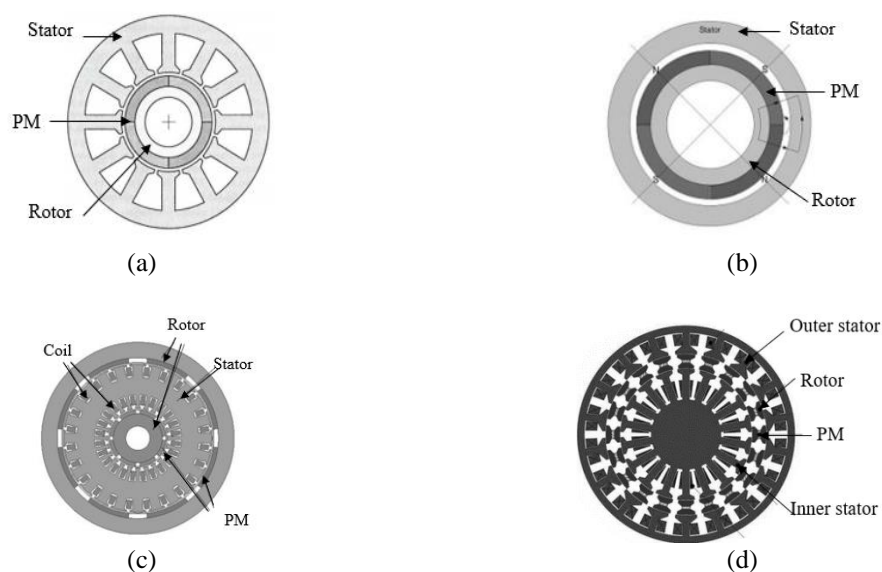


Figure 2. Radial flux orientation PM motors, (a) slotted (single-sided), (b) slotless (single-sided), (c) double rotor, (d) double stator

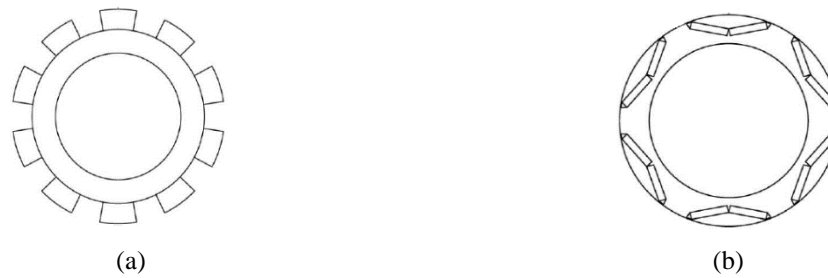


Figure 3. Type of permanent magnet rotor topologies, (a) surface mounted, (b) interior mounted

In other way, axial flux-orientated PM motors construct with flat pancake geometry become a great interest compare to conventional slotted motor design. For axial flux slotted design, high torque density, shorter stack length and high efficiency are achievable instead of radial flux configuration [19-22]. In addition, these motors topologies offer better ventilation and heat removal [23]. Similar to conventional flux topologies, AFPM motors can be construct in single side or double side and with or without slots. For slotted axial flux configuration, the single-sided structure results simple geometry and cheaper but poor torque performance i.e. low torque density, efficiency, unbalanced magnetic force and high cogging torque compare to other axial flux topologies [24]. While, high power-to-weight ratio, low inductance leakages, minimum cogging torque and low vibration can be possible achieved in non-slotted type [25].

Better torque performance can be achieved by having dual-sided configuration i.e. one-stator two-rotor (TORUS) and two-stator-one-rotor (AFIR) design. In many cases, these topologies result high-torque density, balanced magnetic force and high power density instead of single-sided type. In [26], the comparison of TORUS and AFIR motor with slotted and non-slotted configuration are investigated. The slotted TORUS design results high torque density and small electrical loading. While, the AFIR motors results low current density for a similar electrical loading. For non-slotted configuration, both designs may have minimum cogging torque, small torque ripple and low torque ripple than slotted type [27]. However, complex design, severe torque pulsation and low torque density in various on-load situation are inherited compared to conventional motors design [25]. Figure 4 compares variation axial flux orientated configuration in PM motors.

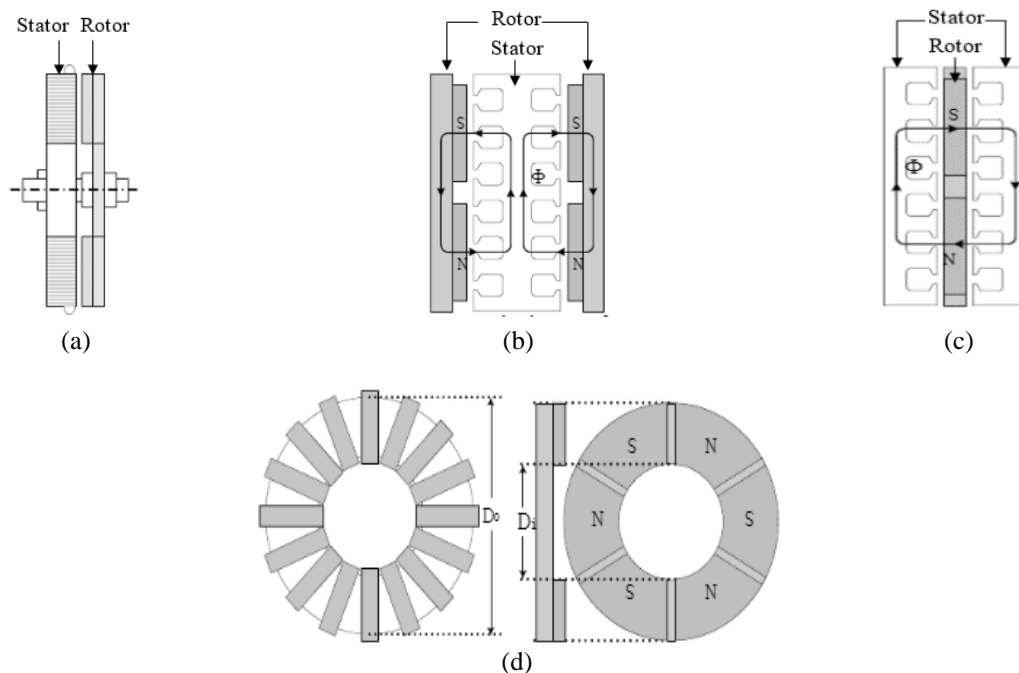


Figure 4. Axial flux orientation PM motors, (a) Single-sided, (b) Interior stator (double-sided), (c) Interior rotor (double-sided), (d) Slotless vs slotted

In this article, further investigation on the developed prototype in [28, 29] via a new asymmetrical stator design is presented aim for overall motor weight reduction and desired torque performance. The approach is applied based on simple technique by removing partial stator design and coil disposition. Influence of parametric designs i.e. narrow tooth body width and additional stator tooth size respectively are included. The investigation is obtained using 2D-Finite Element Analysis.

2. ANALYSIS OF HEMICYCLE STATOR DESIGN

Due to symmetric 3-phase winding mmf vectors, PM motors construct with slot number, N_s is even is a main subject as compared to the motor equips with odd slot number [29]. Influence of various motor design equipped with hemicycle stator design are tabulated in Table 1. The investigation is carried out at 100 rpm rated speed. In term of geometry layout, the stator and permanent magnet are made up of silicon steel and Neodymium Iron Boron (NdFeB) where the magnets are parallelly mounted on outer rotor surface. By having a fixed rotor pole number as tabulated in Table 2 i.e. 10-pole, 6-slots configuration results symmetric winding coil disposition and high winding factor which later no significant drop in behaviour of magnetic performance.

Table 1. Parametric specification over various stator design

Parameter	Specifications			
	Design 1	Design 1 (optimize)	Design 2	Design 3
Model configuration				
Outer stator radius (mm)		60		
Inner stator radius (mm)		36		
Split ratio		0.6		
Tooth body width (mm)	13.1	11.1	11.1	11.1
Coil turn number	104	136	104	136
Additional stator teeth (mm)	0	0	5	5
Stator back iron (mm)		6.7		
Slot depth (mm)		13		
Stack length (mm)		20		
Magnet size (mm)		5		
Airgap thickness (mm)		1		
Slot opening (mm)		1.1		
Tooth tip size (mm)		3.3		
Mode operating		DC		

Table 2. Potential number of slots in asymmetry stator design

Pole number	Conventional		Hemicycle
	Slot number	Winding factor	Slot number
10	6	0.500	6
	9	0.945	
	12	0.933	
	15	0.866	

The idea is based on simple sizing technique by partially remove number of slots i.e. Design 1. Influence of stator tooth body width sizing and copper coil turns is included for a desired output torque performance. Investigation is then extended with 5 mm of additional slot tooth in hemicycle stator design i.e. Design 2 and Design 3 as shown in Figure 5. For Design 2, the additional stator tooth is implemented within 180° which may limit the desired electric loading, slot area and number of coil turns. While, Design 3 are equipped with additional stator tooth over 180° leading to better magnetic flux distribution and output performance for a similar number of coil turns. For winding mmf vectors as shown in Figure 6, the remaining winding belong to phase A, B and C are marked with red, yellow and blue colour respectively. For optimization, all designs are analysed by using 2D-Finite Element Analysis. All designs are applied with 10 A phase current at on-load condition.

By having a proper asymmetrical stator design, Design 3 become main subject of further investigation. As bigger additional stator tooth width size is included, motors theoretically may result better magnetic flux-linkage and offers optimal output torque performance. Investigation is carried out by varying additional slotted tooth from 4 mm to 6 mm while other motor sizing is maintained.

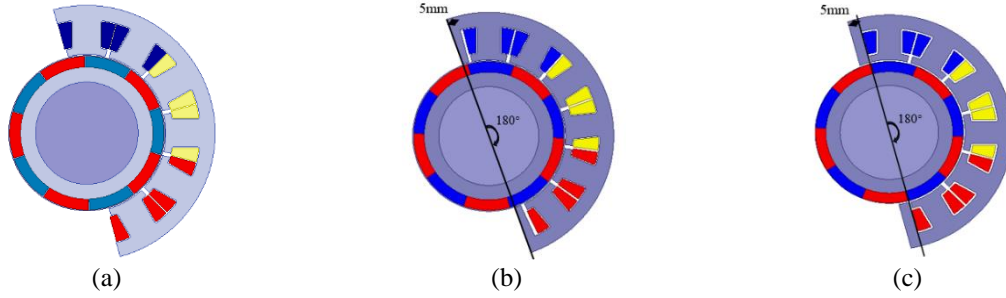


Figure 5. Geometry layout, (a) Design 1 (6-slot), (b) Design 2 (within 180°), (c) Design 3 (over 180°)

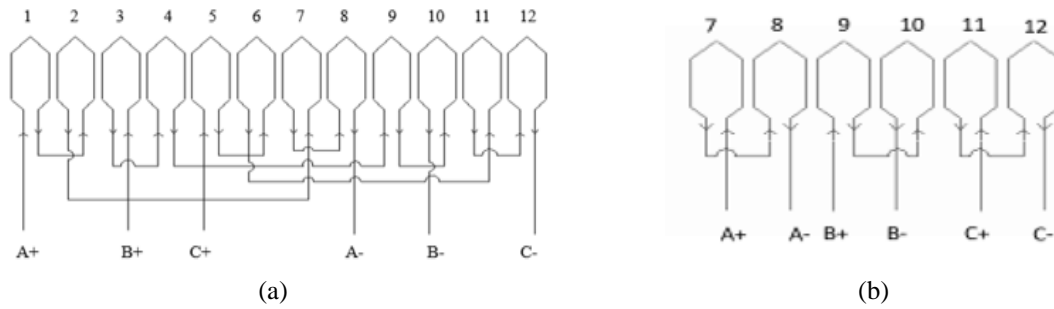


Figure 6. Mmf vectors, (a) conventional (12-slot), (b) Design 1, 2 and 3

2.1. Weight of propose PM motor design

The weight of standard motor design is formulated as follows:

$$W_s = \left\{ \left[\frac{\pi d_{so}^2}{4} - \frac{\pi d_{si}^2}{4} - A_s \right] \times L_a \right\} \times \rho_{ss} \tag{1}$$

$$W_c = \left\{ \left\{ \pi r_c^2 \times [2(S_{tbw} + L_a) \times N_t] \right\} \times N_s \right\} \times \rho_c \tag{2}$$

$$W_m = \left\{ \frac{P_p}{2\pi} \left[\frac{\pi d_{mo}^2}{4} - \frac{\pi d_{mi}^2}{4} \right] \times L_a \right\} \times N_p \times \rho_m \tag{3}$$

where W_s , W_c , W_m is the weight of stator, copper winding and permanent magnet respectively, d_{so} is the outer stator diameter, d_{si} is the inner stator diameter, A_s is the slot area, L_a is the axial length, r_c is the radius of copper coil, S_{tbw} is the tooth body width size, N_t is the number of copper coil, N_s is the number of slot, P_p is the pole-pitch, d_{mo} is the outer rotor magnet, d_{mi} is the inner rotor magnet, N_p is pole-number, ρ_{ss} is the density of silicon steel [7600 kg/m³], ρ_c is the density of copper [8960 kg/ m³] and ρ_m is the density of NdFeB permanent magnet [7400 kg/ m³]. For PM motor equipped with hemicycle stator design i.e. Design 1, the weight of stator body, copper winding and permanent magnet are mathematically derived as follows:

$$W_{sh} = \left\{ \frac{180}{360} \left[\frac{\pi d_{so}^2}{4} - \frac{\pi d_{si}^2}{4} - A_s \right] \times L_a \right\} \times \rho_{ss} \tag{4}$$

$$W_{hc} = \left\{ \left\{ \pi r_c^2 \times [2(S_{tbw} + L_a) \times N_t] \right\} \times N_s \right\} \times \rho_c \tag{5}$$

$$W_{mh} = \left\{ \frac{P_p}{2\pi} \left[\frac{\pi d_{mo}^2}{4} - \frac{\pi d_{mi}^2}{4} \right] \times L_a \right\} \times N_p \times \rho_m \tag{6}$$

where W_{sh} , W_{ch} , W_{mh} is the weight of stator, copper winding and permanent magnet respectively in Design 3. The total weight in proposed motor design is then as derived as follows:

$$W_T = W_s + W_c + W_m \quad (7)$$

The weight comparison in both propose motors design are obtained in term of stator body, copper winding and permanent magnet. For overall motor weight as tabulate in Table 3, the weight of standard motor design is 1.368 kg, it significantly reduce about 44% resulting 0.768 kg in Design 3 via proper sizing of stator body for a desired torque performance.

Table 3. Weight in propose motors design

Pole number	Standard motor	Design 1	Design 2	Design 3
Stator body (kg)	1.032	0.518	0.519	0.556
Copper winding (kg)	0.256	0.098	0.098	0.128
Permanent magnet (kg)	0.08	0.08	0.08	0.08
Total weight (kg)	1.368	0.696	0.697	0.764

3. RESULTS AND ANALYSIS

3.1. Asymmetry end stator teeth

Figure 7 shows the flux-linkages in all designs at no-load condition. With additional stator tooth width, it found better magnetic flux distribution path exist in Design 2 and 3 respectively instead of Design 1. As slot number and size stator width increase, motor theoretically results better magnetic characteristics in term of magnetic loading, flux-linkage, output torque and torque ripple. For back-emf as shown in Figure 8(a), peak back-emf of 3.0 in Design 1 (actual design) rises by 33% equivalent to 4.0 V when additional stator teeth of 5 mm in Design 3 is included. However, no significant change of phase back-emf in Design 2 as the limited slot fill factor and quick saturation condition takes place. All designs are applied with trapezoidal phase current for constant electromagnetic torque. According to Figure 8(b), the rise of higher multiple order harmonic indicates dented peaks and actual Design 1 still results highest back-emf fundamental component. The comparison of permanent magnet flux-linkages in all design are shown in Figure 8(c). The peak flux-linkage in actual design is 0.06 Wb, rise to 0.09Wb with an almost 33% in Design 3. For Design 2, no significant change in peak flux linkage due limited slot area and number of copper turns.

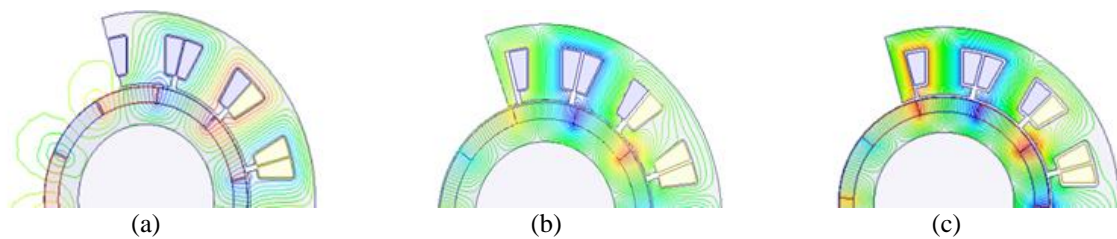


Figure 7. Flux contour at no-load condition, (a) Design 1, (b) Design 2, (c) Design 3

Figure 8(d) compares the peak-to-peak cogging torque at no-load condition. In standard design, motor has maximum cogging torque of 0.96 Nm, it clearly shows no improvement in peak when stator tooth body width is varied i.e. 11.1 mm. For hemicycle motor design, the peak cogging torque significantly reduce by 9.4% and 34% in Design 2 and 3 respectively. It found the cogging cycle increase in Design 3 and this doesn't against with the principle of Lowest Common Multiple, LCM (N_s , $2p$). For static torque performance as shown in Figure 8(e), the average output torque of 4.8 Nm in actual Design 1 rise by 23% equivalent to 5.9 Nm and the torque ripple reduce approximately 50% in Design 3. Besides, Design 3 results six-commutation cycle in one complete electrical cycle and this do not against with standard PM stator design topologies. However, severe situation happens in Design 2 where an average torque is reduced to 3.9 Nm and torque ripple increase to 99%. Hence, Design 3 is the best stator design configuration as it offers better electromagnetic performance, low cogging torque and small torque ripple.

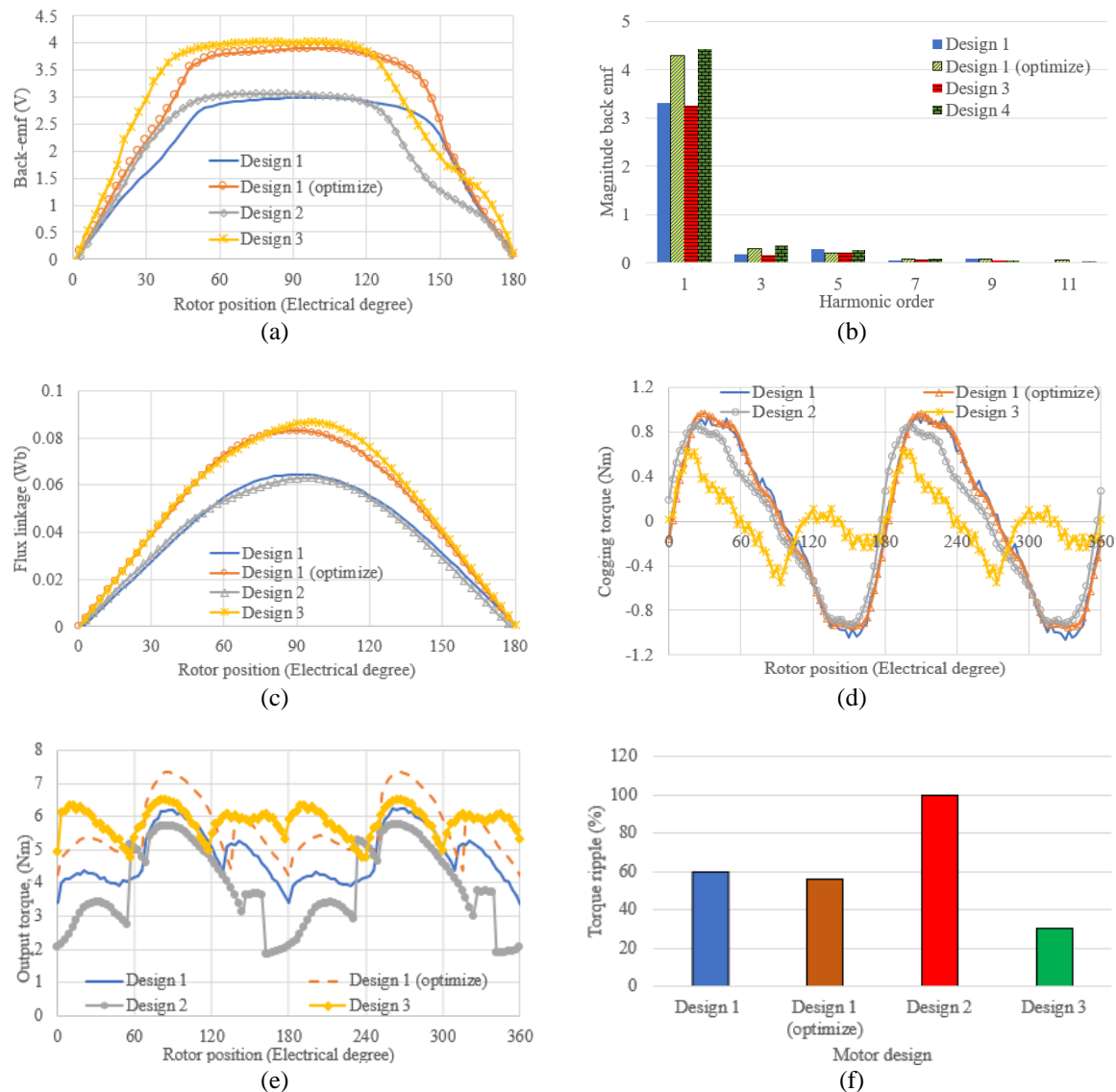


Figure 8. Electromagnetic performance over various stator design, a) phase back-emf, b) harmonics component, c) flux linkage, d) cogging torque, e) output torque, f) torque ripple

3.2. Variation additional end stator tooth

Figure 9(a) compares the maximum phase back emf profile in all design at no-load condition. As narrow tooth body width is included, the peak back-emf in Design 1 (optimize) is 3.9 V rises by 2.6% equivalent to 4 V when additional stator tooth i.e. Design 3 is implemented. It found no significant improvement in peak phase back-emf when additional stator tooth is varied. For harmonic component as shown in Figure 9(b), motor configure with additional stator tooth of 5 mm results the highest fundamental back-emf component. The comparison of flux-linkages in all designs are shown in Figure 9(c). It found there is no significant improvement in peak flux-linkages when additional slotted tooth is varied.

For peak-to-peak cogging torque in Figure 9(d), maximum cogging torque of 0.96 Nm in actual Design 1 reduces by 54% equivalent to 0.44 Nm when additional slots tooth of 5 mm is included. Generally, small cogging torque results small torque ripple and low vibration. In term of electromagnetic torque as shown in Figure 9(e), all designs result a relatively constant in average torque while the torque ripple gradually reduces. It found quick saturation occurs and limits the desired output average torque up to 3.5% only and 30% torque ripple. It is found that the additional slots tooth of 5 mm is the preferable choice. The improve electromagnetic performance via stator modification in PM motor equipped with hemicycle stator design are tabulated in Table 4.

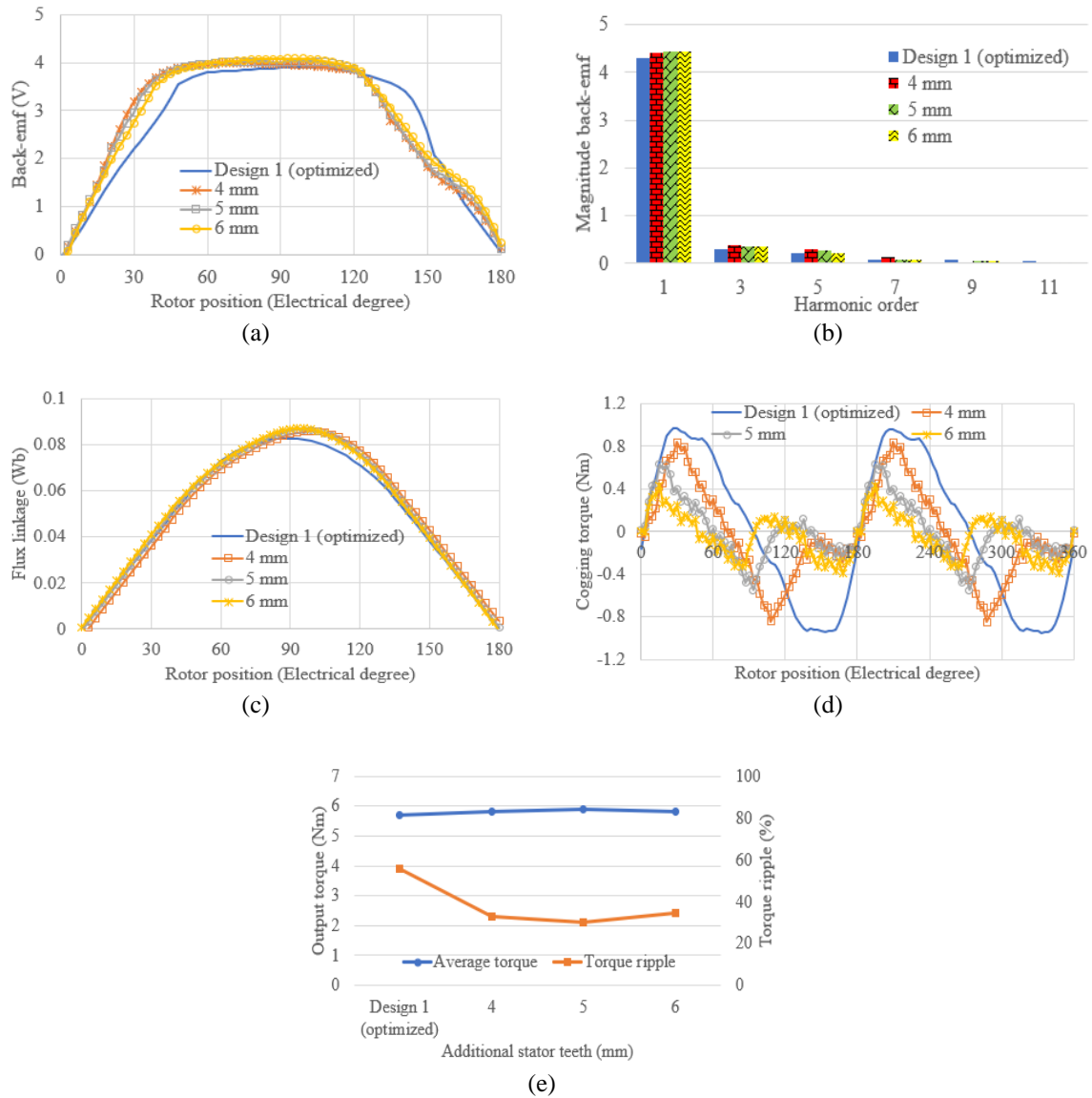


Figure 9. Electromagnetic performance over variation additional stator tooth, (a) Phase back-emf, (b) Harmonics component, (c) Flux linkage, (d) Cogging torque, (e) Electromagnetic output torque

Table 4. Parametric design in propose motor design

Propose method	Configuration	Maximum back-emf (V)	Flux Linkage (Wb)	Maximum cogging torque (Nm)	Average torque (Nm)	Torque ripple (%)
1 Hemicycle stator design	Design 1	3.0	0.06	0.96	4.8	60.0
	Design 1 (optimize)	3.9	0.08	0.96	5.7	55.6
	Design 2	3.0	0.06	0.87	3.9	99.8
	Design 3	4.0	0.09	0.63	5.9	30.0
2 Additional stator tooth (mm) (Design 3)	0	3.9	0.08	0.96	5.7	55.6
	4	4.0	0.09	0.84	5.8	32.8
	5	4.0	0.09	0.63	5.9	30.0
	6	4.0	0.09	0.44	5.8	34.6

4. CONCLUSION

Based on investigation, an overall motor weight can be theoretically decrease by having a proper hemicycle stator geometry. An optimization via proper allocation of stator sizing and number of copper

winding results changes of predicted open-circuit characteristics and static torque. As optimal additional stator tooth size is included, there is a significant improvement in back-emf, output average torque and torque ripple. Due to new torque profile, an intelligent switching is required for future investigation.

ACKNOWLEDGEMENTS

The authors would like to thank Universiti Teknikal Malaysia Melaka (UTeM) for providing the research fund of UTeM Zamalah Scheme.

REFERENCES

- [1] Emadi, A., "Energy Efficient Electric Motors". 3rd ed. 2005, New York: Marcel Dekker.
- [2] Manoj et al, "FEA of a High Efficiency Brushless DC Motor Design," *International Journal of Applied Engineering Research*, vol. 12, no. 1, pp. 11417-11423, 2017.
- [3] Shivraj and Archana, "Mathematical Modelling and Simulation of Three Phase BLDC Motor Using MATLAB," *International Journal of Advance in Engineering & Technology*, 2014; 1426 – 1433.
- [4] Shirish and Jain, "Modelling and Simulation of Three Phase BLDC Motor for Electric Braking Using MATLAB/SIMULINK," *International Journal of Electrical, Electronics And Data Communication*, vol. 5, no. 7, pp. 48-53, 2017.
- [5] Yang M. et al, "A Cost-Effective Method of Electric Brake with Energy Regeneration for Electric Vehicle," *IEEE Transaction on Industrial Electronics*, vol. 56, no. 6, pp. 2203-2212, 2009.
- [6] Talebi et. al., "An Improved Method to Control the Speed of PM-BLDC Motors," *6th International Power Electronics Drive Systems and Technologies Conference*, IEEE Publisher, 3-4 February 2015.
- [7] Seo, J. M. et al, "Design of Axial Flux Permanent Magnet Brushless DC Motor for Robot Joint Module," *The 2010 International Power Electronics Conference*, pp. 1336-1340, 2010.
- [8] Zhou L., Bai S., and Hansen M. R., "Design Optimization on The Drive Train of a Light-weight Robotic Arm," *Mechatronics*, vol. 21, issue 3, pp. 560–569, 2011.
- [9] Amit N. P. et al, "Influence of Difference Type of Stator Slots on Torque Profile of Surface Mounted Pm Motors," *International Journal of Computer Applications in Engineering Sciences*, vol. 5, no. 2, pp. 40-42, 2014.
- [10] Arora A. S. and Gurmeet S., "Review of Design and Performance of Permanent Magnet Synchronous Motor," *Proceeding of The IRES 6th International Conference*, Melbourne, Australia, pp. 107 – 115, 2015.
- [11] Ilka R. et. al., "Design of Slotless BLDC Motor for Elimination Cogging Torque," *Journal of World's Electrical Engineering and Technology*, vol. 3, no. 2, pp. 67-73, 2014.
- [12] Ronghai Q. and Thomas A. L., "Dual-Rotor, Radial-Flux, Toroidally Wound, Permanent Magnet Machines," *IEEE Transactions on Industry Application*, vol. 39, no. 6, pp. 1665-1673, 2003.
- [13] Song S. et. al., "Design and Simulation of Dual Rotor Permanent Magnet Brushless DC Motor," *17th International Conference on Electrical Machines and Systems*, IEEE Publisher, pp. 1591-1595., 2014.
- [14] Pisek P. et. al., "Performance Comparison of Double and Single Rotor Permanent Magnet Machines," *Przegląd Elektrotechniczny*, vol. 87, no 3, pp. 133-136, 2011.
- [15] Swivedi A. and Srivastava R. K., "Analysis of Dual Stator PM Brushless DC Motor," *IOSR Journal of Electrical and Electronics Engineering*, vol. 1, no. 2, pp. 51-56, 2012.
- [16] Firdaus R. N. et. al., "Modelling of torque and speed characteristics of double stator slotted rotor brushless DC motor," *IET Electric Power Applications*, vol. 12, no. 1, pp. 106-113, 2018.
- [17] Firdaus R. N. et. al., "Torque Constant Density in Different Type of Double Stator Permanent Magnet Brushless DC Motor," *Progress in Electromagnetic Research M*, vol. 66, pp. 127-142, 2018.
- [18] J. R. Hendershot & T. J. Miller, "Design of Brushless Permanent Magnet Machines" in Motor Design Books, USA: Florida, 2010.
- [19] Cavagnino A. et al, "A comparison between the Axial Flux and the Radial Flux Structures for PM synchronous Motors," *IEEE Transactions on Industry Applications*, vol. 38, no. 6, pp. 1517-1524, 2002.
- [20] Seo, J. M. et al, "Design of Axial Flux Permanent Magnet Brushless DC Motor for Robot Joint Module," *The 2010 International Power Electronics Conference*, Sapporo, pp. 1336-1340, 2010.
- [21] Guo B. and Huang Y., "A fast-analytic model of axial flux permanent magnet machines with static/dynamic axis eccentricity," *Journal Magnetic*, vol. 21, pp. 554-560, 2016.
- [22] Bouaziz O., et. al., "Performance analysis of radial and axial flux PMSM based on 3D FEM modelling," *Turkish Journal of Electrical Engineering and Computer Sciences*, vol. 26, no. 3, pp. 1587-1598, 2018.
- [23] Mahmoudi A., Rahim N. A., and Hew W. P., "An analytical complementary FEA tool for optimizing of axial-flux permanent magnet machines," *International Journal of Applied Electromagnetics Machines*, vol. 37, no. 1, pp. 19-34, 2011.
- [24] Aydin M. et. al., "Axial Flux Permanent Magnet Disc Machines: A review," Wisconsin Power Electronics Research Centre, September 2004.
- [25] Jacek F. G., Wang R. and Maarten J. K., "Axial Flux Permanent Magnet Brushless Machines," 2nd Edition. Springer, 2008.
- [26] Mahmoudi A., Ping H.W. and Rahim N.A., "A comparison between the TORUS and AFIR axial-flux PM machine using finite element analysis," *Proceeding IEEE International Electrical Machines and Drives Conference-IEMDC 2011*, pp. 242-247, 2011.

- [27] Mahmoudi A., Rahim N. A. and Hew W. P., "TORUS and AFIR axial-flux permanent-magnet machines: A comparison via finite element analysis," *International Review on Modelling and Simulations*, vol. 4, no. 2, pp. 624-631, 2011.
- [28] M. Luqman, Kwang T. C. and Auzani J., "Design and Analysis of PM motor with Semi-circle Stator Design using 2D-Finite Element Analysis," *Indonesian Journal of Electrical Engineering and Computer Science*, vol. 13, no. 1, pp. 427-436, 2019.
- [29] Kwang T. C., Luqman M. and Auzani Jidin, "Torque improvement of PM motor with semi-cycle stator design using 2D-finite element analysis," *International Journal of Electrical and Computer Engineering*, vol. 9, no. 6, pp. 5060-5067, 2019.

BIOGRAPHIES OF AUTHORS



Tan Cheng Kwang was born in Kelantan, Malaysia in 1994 and received the B. Eng degree in Electrical from Universiti Teknikal Malaysia Melaka Malaysia (UTeM), Melaka, Malaysia in 2018. He is currently pursuing his Master of Science at Universiti Teknikal Malaysia Melaka, Malaysia.



Mohd Luqman Mohd Jamil received the B.Eng. degree from the Universiti Teknologi MARA, Shah Alam, Malaysia, in 2000, the M.Sc. degree from Newcastle University, Newcastle upon Tyne, U.K., in 2003, and the Ph.D. degree from The University of Sheffield, Sheffield, U.K., in 2011, all in electrical engineering. He is currently an academician with the Department of Power Electronics and Drives, Faculty of Electrical Engineering, University Teknikal Malaysia Melaka, Melaka, Malaysia. His research interests include the design and analysis of permanent-magnet brushless machines.



Auzani Jidin received his B. Eng, M. Eng. And Ph.D, in Power Electronics and Drives from Universiti Teknologi Malaysia (UTM), Johor, Malaysia in 2002, 2004 and 2011 respectively. He is an academician in Department of Power Electronics and Drives, Faculty of Electrical Engineering, Universiti Teknikal Malaysia Melaka Malaysia. His research interest includes the field of power electronics, motor drives systems, field programable gate arrays and digital signal processing applications.